frontiers in Mechanical Engineering

REVIEW
published: 05 February 2019
doi: 10.3389/fmech.2019.00002

Macroscale Superlubricity Achieved With Various Liquid Molecules: A Review

Xiangyu Ge, Jinjin Li and Jianbin Luo**

State Key Laboratory of Tribology, Tsinghua University, Beijing, China

Superlubricity is generally classified as solid superlubricity and liquid superlubricity according to the lubricants involved at the interfaces, and is a popular research topic in tribology, which is closely linked to energy dissipation. Significant advancements in both experimental studies and theoretical analysis have been made regarding superlubricity in the past two decades. Compared with solid superlubricity, liquid superlubricity has many advantages; e.g., it is more easily achieved at the macroscale and less sensitive to the surface smoothness and atmospheric conditions. In the present study, the advancements in liquid superlubricity at the macroscale are reviewed, and the corresponding mechanisms for various types of liquid lubricants are discussed. This investigation is important for engineering traditional mechanical lubricating systems. Finally, the issues regarding the liquid superlubricity mechanism and the future development of liquid superlubricity are addressed.

Keywords: macroscale superlubricity, liquid lubricants, polymers, acid-based lubricants, room-temperature ionic liquids, oil-based lubricants, nanomaterial-based lubricants

OPEN ACCESS

Edited by:
Valentin L. Popov,
Technische Universität Berlin,
Germany

Reviewed by:
Wenling Zhang,
University of Alberta, Canada
Ali Erdemir,
Argonne National Laboratory (DOE),
United States

****Correspondence:***
Jinjin Li
lijinjin@mail.tsinghua.edu.cn
Jianbin Luo
luojb@tsinghua.edu.cn

Specialty section:
This article was submitted to Tribology, a section of the journal Frontiers in Mechanical Engineering

Received: *17 December 2018*
Accepted: *17 January 2019*
Published: *05 February 2019*

Citation:
Ge X, Li J and Luo J (2019) Macroscale Superlubricity Achieved With Various Liquid Molecules: A Review. Front. Mech. Eng. 5:2. doi: 10.3389/fmech.2019.00002

INTRODUCTION

Because the energy consumption and material losses derived from friction and wear in mechanical systems place large economic and environmental burdens on all nations (Erdemir and Eryilmaz, 2014), studies on lubrication technology and mechanisms are very important for energy conservation and emission reduction. Since it was invented in the early 1990s (Shinjo and Hirano, 1993), superlubricity has attracted extensive concentration from researchers in many fields (Tisza, 1938; Meyer and Gnecco, 2014; Baykara et al., 2018; Li et al., 2018a,b). It describes a phenomenon where the friction force between two sliding surfaces nearly vanishes ideally (Hirano, 2014) or a state in which the sliding coefficient of friction (COF) is <0.01 in actual mechanical lubricating systems (Erdemir et al., 2007).

Superlubricity is generally classified as solid superlubricity and liquid superlubricity according to the lubricants involved at the interfaces (Baykara et al., 2018; Berman et al., 2018; Sinclair et al., 2018). Solid superlubricity at the nanoscale or microscale is easily achieved with two-dimensional materials, such as molybdenum disulfide (Martin et al., 1994), graphite flakes (Liu et al., 2012), boron nitride (BN) (Song et al., 2018), and graphene (Feng et al., 2013). It has also been achieved at dissimilar interfaces, including the crystalline gold/graphite interface (Cihan et al., 2016), graphene nanoribbons/gold interface (Kawai et al., 2016), and silica/graphite interface

(Li et al., 2018a). However, solid superlubricity at the macroscale is rarely achieved (Li et al., 2018b), owing to the strict requirement of atomically smooth contact in these materials. In contrast to solid superlubricity, many liquid lubricants have been found to possess a macroscale superlubricity property, such as water (Xu and Kato, 2000; Zhou et al., 2005), oils (Bouchet et al., 2007; Matta et al., 2008), and polymers (Muller et al., 2003; Zhang et al., 2017). The superlubricity mechanism of these lubricants accounts for the formation of a hydrogen-bond network, a tribofilm, a hydration layer, or a molecular brush, depending on the properties of the lubricants. Recently, our group found that a phosphoric acid aqueous solution ($H_3PO_{4(aq)}$) as a liquid lubricant could achieve superlubricity at the Si_3N_4/SiO_2 interface with an extremely low COF of 0.004 under maximum initial contact pressures of 700 MPa (Li et al., 2011, 2012, 2013a). According to the superlubricity mechanism of $H_3PO_{4(aq)}$, a series of acid-based lubricants composed of different polyhydroxy alcohols and acids were established (Li et al., 2013b,c). Among these acid-based lubricants, the one composed of polyethylene glycol (PEG) and boric acid (BA) allows superlubricity to be achieved under neutral conditions, avoiding acid corrosion (Ge et al., 2018a). Room-temperature ionic liquids (RTILs) are well-known as eco-friendly lubricants and lubricating additives (Ge et al., 2015; Jiang et al., 2018). Research into the superlubricity property of RTILs has been performed by experts recently (Espinosa et al., 2014). Because RTILs can be designed by combining a variety of cations and anions, it is possible to develop RTILs possessing not only the superlubricity property but also special properties for different operating conditions. One of the issues for liquid lubricants is that the wear is severe during the wearing-in period. To alleviate this defect, a mixture of short-chain dihydric alcohol and graphene-oxide nanoflakes (GONFs) is explored, making it possible to achieve macroscale superlubricity and super-low wear simultaneously.

To better illustrate the differences of the superlubricity materials and their corresponding superlubricity mechanisms, these superlubricity materials are classified into 6 main types based on the main functioning materials during superlubricity period. The "Water" section describes the first discovery of superlubricity at a ceramic interface. The "Polymers" section reviews the superlubricity property of polymers. The "Acid-Based Aqueous Lubricants" section presents the development of a single phosphoric acid into a series of acid-based lubricants composed of acids and polyhydroxy alcohols. The "RTIL Lubricants" section outlines recent advances in RTILs, focusing on their superlubricity mechanism. The "Oil-Based Lubricants" section describes the superlubricity achieved with oils and oil-like liquids. The "Nanomaterial-Based Lubricants" section focuses primarily on the feasibility of macroscale superlubricity achieved with nanomaterials (like GONFs, BN, NaOH-modified black phosphorus (BP-OH), layered double hydroxide nanoplatelets (LDH), and nanodiamonds) as additives. The "Conclusions and Outlooks" section concludes the paper, offering perspectives and suggestions for future research on macroscale liquid superlubricity.

WATER

The first liquid superlubricity phenomenon was discovered by Tisza with helium II in 1938 (Tisza, 1938); it was called superfluidity at that time. In 1987, water was found to provide superlubricity at the Si_3N_4/Si_3N_4 interface, and an extremely low COF—even <0.002—was achieved after a wearing-in period (Tomizawa and Fischer, 1987). The wearing-in process provides ultra-smooth surfaces and a very low contact pressure. The smooth surfaces make the lubrication enter the elastohydrodynamic lubrication (EHL) regime, in which a thin water film exists at the interface and provides low viscous friction. In addition to smooth surfaces, tribochemical reactions contribute to the superlubricity. Induced by shear, a tribochemical film is formed on the surfaces via tribochemical reactions, as indicated by Equations (1, 2) (Spikes and Tysoe, 2015; Khajeh et al., 2018). This film has extremely low shear resistance and can be maintained on the surfaces during the rubbing process. Analysis shows that this tribofilm is composed of colloidal silica, which can produce the electrical double layer, leading to very low friction in boundary lubrication (BL). Therefore, an extremely low friction is achieved in the mixed lubrication (ML) regime (EHL + BL) under a low contact pressure. Later, several studies on ceramic lubrication, e.g., using SiC, were performed under water lubrication (Chen et al., 2001, 2002). These studies report that the COFs under water lubrication can decrease to 0.01 or even less, but the wearing-in period is significantly longer than that for a Si_3N_4/Si_3N_4 tribopair, as depicted in **Figure 1**. Their superlubricity mechanism is similar to that of Si_3N_4/Si_3N_4 tribopairs: the large friction reduction results from the decrease of the contact pressure and the formation of the colloidal silica tribofilm as indicated by Equations (2, 3).

However, there are two issues for ceramic tribopairs under water lubrication. First, the wear on ceramic surfaces is too large. To solve this issue, amorphous carbon nitride coatings (a-CN_x) are deposited on the surface of a Si_3N_4 disc. For an a-CN_x/ Si_3N_4 tribopair, after a wearing-in period under water lubrication, an average stable COF of ∼0.007 is achieved at a sliding speed of 160 mm/s and a normal load of 5 N (Zhou et al., 2007). Moreover, the wear rate of the Si_3N_4 ball in an a-CN_x/Si_3N_4 tribopair is only 1/35 of that in a Si_3N_4/Si_3N_4 tribopair under water lubrication. The wear mechanism of a-CN_x/Si_3N_4 is the formation of a carbonaceous transfer film on the a-CN_x coatings via a tribochemical reaction between the a-CN_x coatings and water induced by friction. The second issue is that the superlubricity of ceramic tribopairs under water lubrication can hardly be achieved under a high contact pressure; thus, laser texturing technology is applied to SiC/SiC tribopairs to improve the load-carrying capacity of their surfaces (Wang et al., 2001). The critical load, under which the COF suddenly increases, is used to evaluate the effect of the surface texture, and a high critical load indicates that the load-carrying capacity is high. The authors conclude that the optimum pore area ratio (the ratio of the area occupied by pores to the area of the end surface) is 2.8% for SiC for providing the highest critical load, which is 20% higher

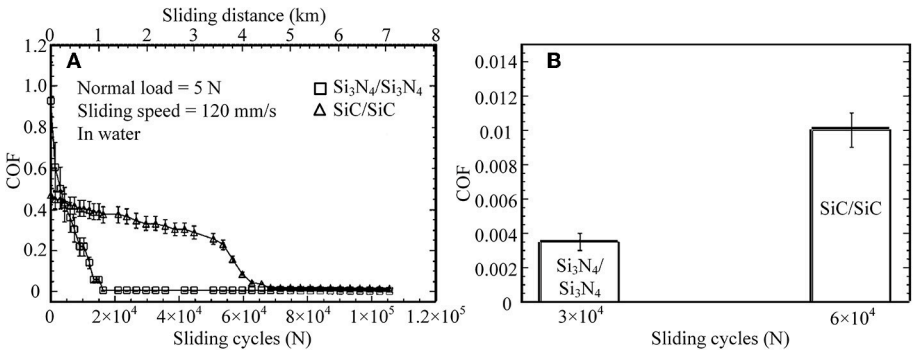

FIGURE 1 | (A) COFs for various sliding cycles and sliding distance, **(B)** average COFs for various sliding cycles. Si_3N_4/Si_3N_4 and SiC/SiC tribopairs under water lubrication: the normal load is 5 N, the sliding speed is 120 mm/s. Chen et al. (2001) Copyright 2001, Springer.

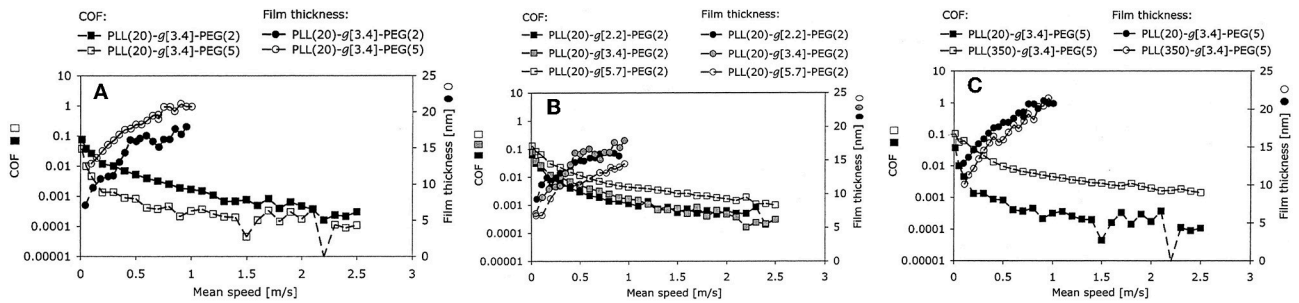

FIGURE 2 | Effects of **(A)** the molecular weight of the PEG side chains, **(B)** the Lys/PEG grafting ratio, and **(C)** the molecular weight of the PLL backbone on the COF. The lubricant film thickness was measured with respect to the speed using an MTM and ultrathin-film interferometry. Muller et al. (2003) Copyright 2003, Springer.

than that of the untextured SiC surface (Wang et al., 2001).

$$Si_3N_4 + 6H_2O \rightarrow 3SiO_2 + 4NH_3 \quad (1)$$

$$SiO_2 + 2H_2O \rightarrow Si(OH)_4 \quad (2)$$

$$SiC + 2H_2O \rightarrow SiO_2 + CH_4 \quad (3)$$

POLYMERS

Because they can be both solid-like to sustain a normal load and liquid-like to shear easily (Baykara et al., 2018), polymers are usually grafted onto contact surfaces to form polymer brushes, which can be adsorbed on the charged surfaces via electrostatic adsorption, and are accompanied by good solvents for achieving superlubricity. For instance, the copolymer poly(L-lysine)-g-poly(ethylene glycol) (PLL-g-PEG) can be synthesized by grafting PEG onto poly(L-lysine) (PLL) and has proven to be an effective biomimetic BL additive in aqueous lubrication (Lee et al., 2003). An extremely low COF of 0.0001 was achieved on a mini-traction machine (MTM), which allows rolling friction testing; thus the hydrodynamic effect is very strong (Muller et al., 2003). The influence of the chemical architecture on the lubricity performance has been studied in detail, including the side-chain (PEG) length, Lys/PEG grafting ratio, and backbone chain (PLL) length, as depicted in **Figure 2**. The authors demonstrate that both the increase of the molecular weight of PEG and the reduction of the grafting ratio enhance the lubricity properties of the aqueous PLL-g-PEG solution at low sliding velocities, and the increase of the molecular weight of the PLL leads to an increase of the COF. The superlubricity mechanism for a neutral brush is as follows: the permeation pressure of the solvent makes the PEG chains spread throughout the aqueous solution, leading to the formation of molecular brushes and the separation of the contact surfaces, which can greatly reduce the friction (Raviv et al., 2003). A solvent layer with low shear resistance between the brush layers helps to achieve superlubricity (Klein, 2013). The superlubricity mechanism of a charged brush is similar to that of a neutral brush at low pressures. However, at high pressures, the permeation pressure of the trapped counter-ions provides extra load support, while the hydration layer formed between the two polymer surfaces provides low friction (Raviv et al., 2003; Inutsuka et al., 2013; Klein, 2013; Ron et al., 2016), thereby improving the performance of the charged brush compared with a neutral brush.

Recently, researchers reported a new grafting method for acquiring hydrophilic polymer brushes on poly(dimethyl siloxane) (PDMS) surfaces (Ron et al., 2016). This method is based on the selective separation of the hydrophilic chain in an amphiphilic diblock copolymer under water conditions, as depicted in **Figure 3**. The amphiphilic diblock copolymers can be formed by charged hydrophilic poly(acrylic acid) (PAA) and PDMS or by neutral PEG and PDMS and are denoted

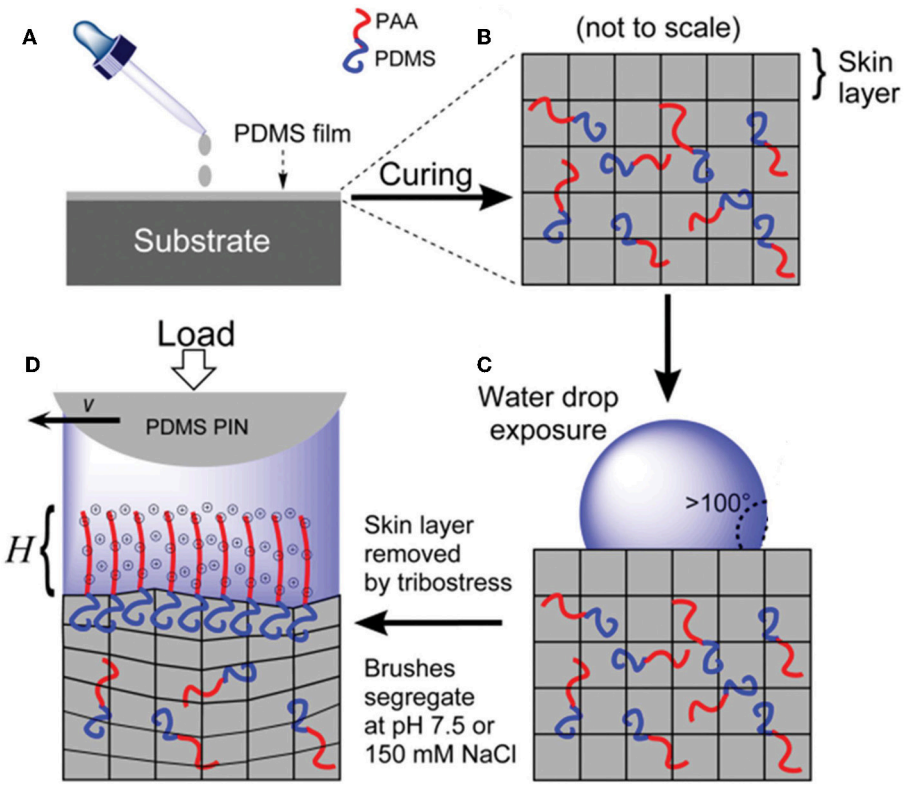

FIGURE 3 | (A) Coating of a substrate with a PDMS film. **(B)** Crosslinked PDMS matrix incorporating diblock copolymers and a skin layer. **(C)** High water contact angle is attributed to the PDMS skin layer formation. **(D)** Tribostress shears off the skin layer and induces brush segregation with charges and counter ions. H is the brush height. Ron et al. (2016) Copyright 2015, Wiley-Vch Verlag GmbH and Co. KGaA, Weinheim.

as PDMS-b-PAA and PDMS-b-PEG, respectively. This grafting strategy causes the polymer brushes to be regenerated *in situ*. For instance, when the brush layer is damaged under harsh operating conditions, it can be readily self-restored without any external supports. This self-restoring feature makes it very useful for lubricating systems, because the stability and durability of lubricants are very important for a steady lubricating performance. Friction test results show that under different conditions, including the substrate, load, counter surface, pH, and salinity, the COFs of these two polymer brushes are between 0.001 and 0.05 for soft contacts. Moreover, charged PAA exhibits far better lubricity than neutral PEG, which is explained by the significantly lower free energy of the PAA chains upon hydration.

Recently, poly(vinylphosphonic acid) (PVPA) with salt ions was found to achieve superlubricity on a Ti_6Al_4V/polytetrafluoroethylene tribopair. Research into the superlubricity mechanism reveals that the cations and anions function together to achieve the superlubricity even under harsh conditions (Zhang et al., 2017). This finding makes PVPA-modified Ti_6Al_4V a potential material for artificial implants. It is concluded that when used as lubricants, polymers must be accompanied by a good solvent. In this way, solvent molecules can improve the stretching of polymer brushes for inducing a permeation pressure to sustain a normal load and provide low friction.

Similar to polymers, macroscale superlubricity could be achieved with hydrated alkali metal ions (Li^+, Na^+, K^+) based on hydration effect (Han et al., 2018). This superlubricity is attributed to the hydration layer formed by alkali metal ions, providing hydration repulsive force and having a liquid-like response to shear. This work paves the way to the macroscale superlubricity induced by hydration effect and therefore to the wide application of hydration lubrication.

ACID-BASED AQUEOUS LUBRICANTS

Phosphoric acid as a lubricant was first found to achieve superlubricity at the Si_3N_4/glass interface in 2011 (Li et al., 2011). Thereafter, acid-based lubricants as a new series of lubricants were investigated by the authors in detail at various tribopairs, such as Si_3N_4/glass, Si_3N_4/SiO_2, Si_3N_4/sapphire, and ruby/sapphire (Deng et al., 2014; Li et al., 2014). As depicted in **Figure 4a**, when a Si_3N_4 ball slides on a glass disc under the lubrication of $H_3PO_{4(aq)}$, the COF decreases from 0.45 to 0.004 after a wearing-in period of 600 s. The wearing-in period is vital to the achievement of superlubricity and can be divided into two stages according to the evolution of the COF with time. In each wearing-in stage, a different mechanism accounts for the friction reduction.

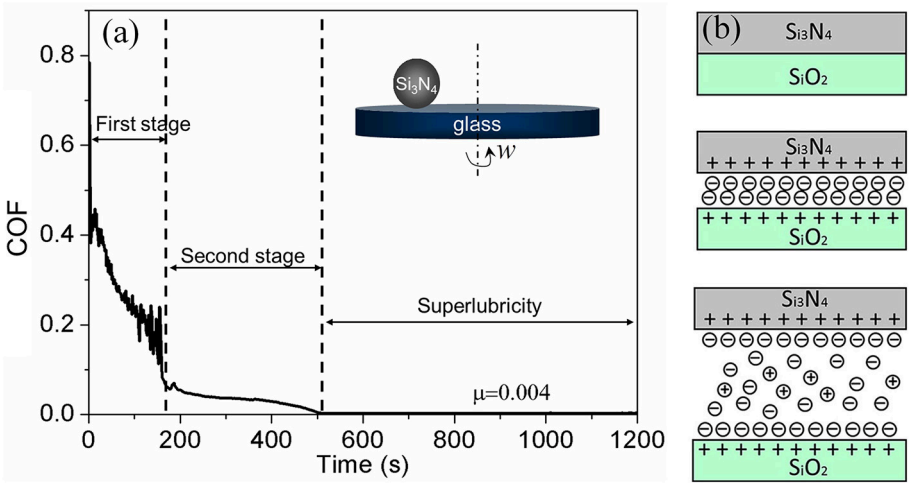

FIGURE 4 | (a) Evolution of the COF with time under lubrication with an H_3PO_4 aqueous solution (pH = 1.5). Inset is the ball-on-disk model for friction testing. The tribopair is Si_3N_4/glass, the load is 3 N, and the sliding velocity is 75 mm/s. (Li et al., 2013a) Copyright 2013, AIP Publishing LLC. **(b)** Schematic of the lubrication model, including three kinds of contacts. Li et al. (2012) Copyright 2012, American Chemical Society.

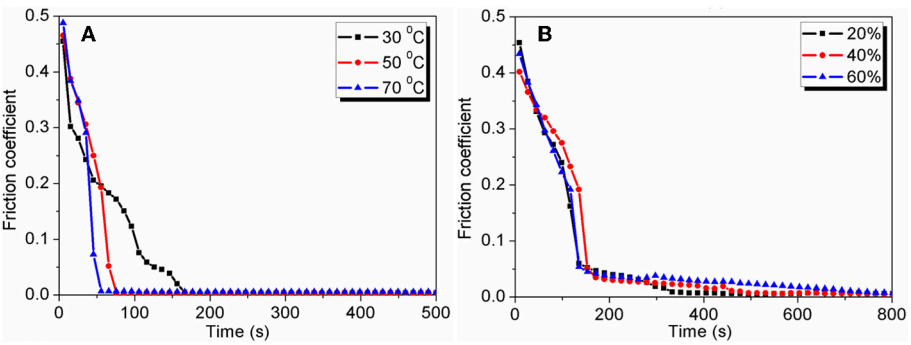

FIGURE 5 | Effects of the temperature and humidity. **(A)** Evolution of the COF with time under lubrication with H_3PO_4 (pH = 1.5) at different temperatures, at a humidity of 25%. **(B)** Evolution of the COF with time under lubrication with H_3PO_4 (pH = 1.5) at different humidity values, at a temperature of 25°C. The tribopair is Si_3N_4/glass, the load is 3 N, and the sliding velocity is 75 mm/s.

In the first wearing-in stage, H^+ ions play a key role in the rapid reduction of the COF from 0.45 to 0.05. Because there are ≡ SiOH bonds on the surfaces of glass and Si_3N_4, the H^+ ions in H_3PO_4 can be adsorbed on the contact surfaces via the protonation reaction (Sjoberg, 1996; Sahai, 2002), making the contact surfaces become positively charged after the first wearing-in stage. The surface charge is balanced by $H_2PO_4^-$ anions; therefore, a stern layer and diffuse double layer form between the two charged surfaces (**Figure 4b**), which provide a repulsive force and a hydration force, respectively. With the increase of the contact area, which is caused by wear, the contact pressure decreases. After the first wearing-in stage, the contact pressure, hydration force, and repulsive force are in an equilibrium state, leading to significant friction reduction.

Although H^+ ions strongly affect the friction reduction in the first wearing-in stage, they cannot realize superlubricity directly. Among the acids, only H_3PO_4 is found to realize superlubricity after the second wearing-in stage; the COF decreases from 0.05 to 0.004 gradually. For other acids, there is no second wearing-in stage, and the COF remains larger than 0.01 (Li et al., 2012), indicating that the second wearing-in stage is unique to H_3PO_4. H_3PO_4 is in a liquid state before the end of second wearing-in stage, when only a solid-like layer is observed on the wear track. This is because the free water evaporates completely from the lubricant at the end of the second wearing-in stage, resulting in only hydrated water molecules remaining in the solid-like layer. Thus, the second wearing-in stage is closely related to the water evaporation, which has been experimentally proven at different temperatures and humidities, as depicted in **Figure 5**. At a lower temperature or a higher humidity, a longer wearing-in period is needed to vaporize the water completely. The chemical composition of the solid-like layer is investigated using Raman spectroscopy, which shows that the solid-like layer is composed of the hydrogen-bond network of H_3PO_4 and

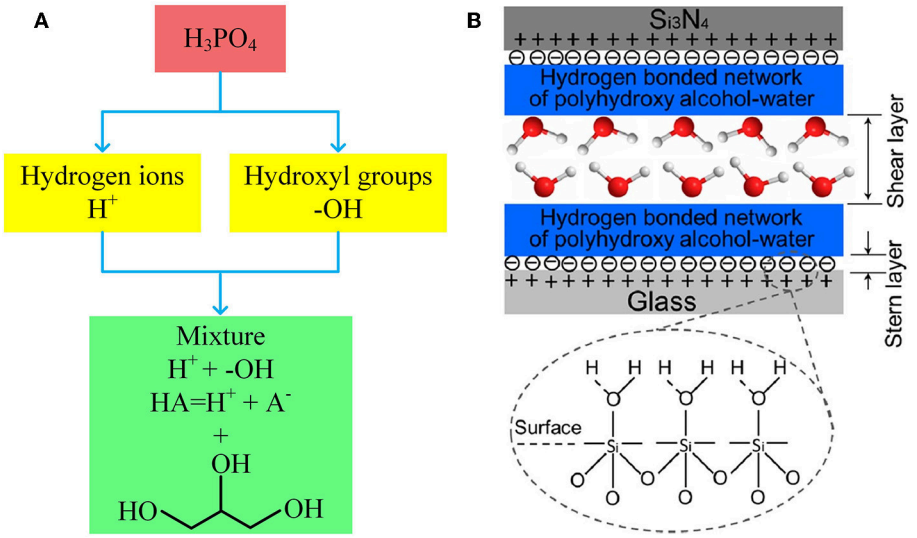

FIGURE 6 | (A) Illustration of promoting phosphoric acid to a mixture of glycerol and acid. **(B)** Schematic of the possible lubrication model between the two friction surfaces. The red and white spheres represent oxygen and hydrogen atoms, respectively. Li et al. (2013c) Copyright 2013, American Chemical Society.

hydrated water molecules (Li et al., 2013a). If the hydrogen-bond network is destroyed by adding 2 μL of pure water to the wear track, the superlubricity state is destroyed immediately (Li et al., 2011), indicating that the superlubricity is closely related to the hydrogen-bond network. Moreover, the low friction state of phosphoric acid was simulated by reactive molecular dynamics (Yue et al., 2013). The simulation result at a temperature between 300 and 600 K shows no tribochemical reaction occurred, and the COF reduced due to the acceleration in both rotational- and translational-motions of lubricant molecules and the weakened hydrogen-bond network.

Based on the foregoing analysis, the superlubricity model of H_3PO_4 is proposed. In the first wearing-in stage, H^+ and $H_2PO_4^-$ ions are adsorbed on the contact surfaces, forming the stern layer. After the second wearing-in stage, the hydrogen-bond network is adsorbed above the stern layer and plays a key role in sustaining load. In addition to providing load support, an important function of the hydrogen-bond network is locking water molecules in the contact region. It is inferred that a thin hydrated water layer is adsorbed on the surface of the hydrogen-bond network because of the strong hydrogen-bond effect of the H_3PO_4 molecules, similar to a water layer adsorbed on the top of surface of ice (Dash et al., 1995). During sliding, shearing occurs in the hydrated water layer because of its good fluidity under a high pressure (Klein, 2013).

The superlubricity model of H_3PO_4 indicates that this type of superlubricity is dominated by two factors: the positively charged surfaces formed by the adsorption of H^+ ions and the hydrogen-bond network of H_3PO_4 and water molecules. Accordingly, it is possible to achieve superlubricity with a mixture of acid and polyhydroxy alcohol, because the H^+ ions from the acid can satisfy the first factor and the hydroxyl groups from the polyhydroxy alcohol can satisfy the second factor, as depicted in **Figure 6A**.

TABLE 1 | Lowest COF under lubrication with four kinds of polyhydroxy alcohols and their mixtures with four kinds of acid lubricants (H_2SO_4, HCl, $H_2C_2O_4$, and H_3NO_3S, pH = 1).

	No acid	H_2SO_4	HCl	$H_2C_2O_4$	H_3NO_3S
1,2-ethanediol	0.05	0.004	0.004	0.004	0.003
1,3-propanediol	0.07	0.004	0.003	0.003	0.003
1,4-butanediol	0.06	0.004	0.005	0.005	0.004
1,5-pentanediol	0.06	0.004	0.006	0.004	0.003

The tribopair is Si_3N_4/glass, the load is 3 N, and the sliding velocity is 75 mm/s. Data are obtained from Li et al. (2013c), Copyright 2013, American Chemical Society.

To prove this hypothesis, mixtures of acids (H_2SO_4, HCl, $H_2C_2O_4$, and H_3NO_3S, pH = 1) and polyhydroxy alcohols (glycerol, 1,2-ethanediol, 1,3-propanediol, 1,4-butanediol, and 1,5-pentanediol) were prepared and tested. If the tests are performed with these polyhydroxy alcohols only, the minimum COF would be larger than 0.05. If the tests are performed with the mixtures, the friction behavior of the mixtures is similar to that of H_3PO_4: the COF decreases to ~0.05 during the wearing-in period and then gradually decreases to <0.01 (Li et al., 2013b,c). The minimum COFs of these mixtures are listed in **Table 1**, indicating that superlubricity can be achieved by the mixtures of acids and polyhydroxy alcohols.

The superlubricity of these mixtures is affected by the concentration of polyhydroxy alcohol in the mixture. Superlubricity can be achieved if the concentration of polyhydroxy alcohols is less than a critical value, which is 40, 50, 40, and 30% for 1,2-ethanediol, 1,3-propanediol, 1,4-butanediol, and 1,5-pentanediol, respectively. The superlubricity mechanism of these acid-based mixtures is as follows: the hydrogen-bond network formed by polyhydroxy alcohols and water molecules is adsorbed onto the surface of the stern layer (induced by H^+ ions) during the wearing-in period; thus,

a hydrated water layer is formed, yielding superlubricity, as depicted in **Figure 6B** (Li et al., 2013c).

To check whether all the alcohols can be mixed with acid to achieve superlubricity, three key characteristics of alcohols that affect their physicochemical properties are investigated: the number of hydroxyl groups, the position of the hydroxyl groups on the C-C skeletal chain, and the length of the C-C skeletal chain (Li et al., 2013c). **Figure 7A** shows the friction results for lubrication with four mixtures of alcohols (1-propanol, 2-propanol, 1,2-propanediol, and 1,3-propanediol) and H_2SO_4 (pH = 1). Clearly, the mixtures formulated with 1-propanol and 2-propanol cannot achieve superlubricity. Because there is only one hydroxyl group in 1-propanol and 2-propanol and there are two or three hydroxyl groups in the other three kinds of alcohols, there should be at least two hydroxyl groups in the structure for achieving superlubricity. Moreover, comparing the result for 1,2-propanediol with that for 1,3-propanediol reveals that the position of the hydroxyl groups hardly affects the superlubricity. The effect of the length of the carbon chain is tested with mixtures of H_2SO_4 and five other polyhydroxy alcohols: ethylene glycol, diethylene glycol, triethylene glycol, tetraethylene glycol, and pentaethylene glycol, which have 2, 4, 6, 8, and 10 carbon atoms in the C-C skeletal chain, respectively. The results in **Figure 7B** indicate that superlubricity can be achieved by all five mixtures and that the length of the C-C skeletal chain has no obvious effect on the superlubricity (Li et al., 2013c).

As mentioned previously, the two factors for superlubricity are the H^+ ions and the hydrogen-bond network. The first factor can be satisfied for all mixtures because of the existence of acid, but if the alcohol has only one hydroxyl group in its molecular structure, it cannot form a hydrogen-bond network with water molecules and thus cannot satisfy the second factor for superlubricity. If the alcohol has more than one hydroxyl group in its molecular structure, it can form the hydrogen-bond network with water molecules, yielding superlubricity. The position of the hydroxyl groups and the number of carbon atoms in the C-C skeletal chain have no effect on the hydrogen-bond network formation and thus have no obvious effect on the superlubricity.

Analysis of the superlubricity behavior of H_3PO_4 and the mixtures of polyhydroxy alcohols and acids reveals that their superlubricity mechanism is the same and that the two critical factors for superlubricity are the H^+ ions and the hydrogen-bond network. The H^+ ions help to form the stern layer on the surfaces via the protonation reaction, which requires the pH of the lubricant to be <2. The hydrogen-bond network provides load support and locks water molecules in the contact region, which requires the existence of at least two hydroxyl groups in the lubricant molecular structure. The authors proved that these two factors are required for achieving superlubricity. The steady COF achieved with only H^+ ions (e.g., acid, except for H_3PO_4) is >0.03, and that achieved with only the hydrogen-bond network (e.g., glycerol only) is >0.02. The superlubricity mechanism of the acid-based lubricants is attributed to both the formation of the hydrogen-bond network and the stern layer. The friction results and mechanism indicate that if a liquid lubricant satisfies two criteria—possessing H^+ ions (pH $\leq$ 2) and at least two hydroxyl groups in its molecule—liquid superlubricity can be achieved. Therefore, a novel system of liquid superlubricity based on H^+ ions and hydroxyl groups is established, and this study offers a new method for achieving liquid superlubricity.

However, the strong acidity of these acid-based lubricants limits their applications in a practical mechanical system. Recently, a new type of acid-based lubricant, which is a mixture of BA and a PEG aqueous solution ($PEG_{(aq)}$), was synthesized and found to provide superlubricity (COF $\approx$ 0.004) in neutral conditions (pH $\approx$ 6.4) at Si_3N_4/SiO_2 interfaces, as depicted in **Figure 8** (Ge et al., 2018a). The mechanism of this superlubricity achieved in neutral conditions is similar to that of acid-based lubricants discussed previously. The neutral condition is attributed to the tribochemical reactions (Equation 4) between PEG (denoted as HOROH, where R is the alkyl chain) and BA (Shteinberg, 2011), which can provide sufficient H^+ to form the stern layer and to reduce the friction during the wearing-in period. The H^+ then can be consumed by further reaction (Equation 5) with NH_3 from the reaction of Equation (1) to maintain a neutral condition (Shteinberg, 2009). Furthermore, a tribochemical layer is formed on the contact surfaces to provide low friction. Such liquid superlubricity achieved in neutral conditions is of immense importance to both scientific understanding and industrial technology implementation.

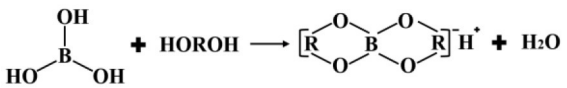

(4)

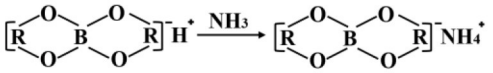

(5)

RTIL LUBRICANTS

RTILs are a series of well-known lubricants and lubricant additives in surface science and engineering (Ye et al., 2001; Qu et al., 2012, 2015) because they can improve the lifetime of mechanical systems by reducing the friction and providing wear protection (Holmberg et al., 2012). The tribological properties of RTILs, such as the friction reduction, anti-wear, and anti-corrosion properties, have been well explored (Somers et al., 2013; Fan et al., 2014; Saurin et al., 2016; Li et al., 2017). However, studies of the superlubricity of RTILs have only been performed under a very low normal load (0.02 N) in combination with carbon quantum dots (Ma et al., 2017), or at the microscale between a SiO_2/graphite tribopair (Li et al., 2014). Therefore, the macroscale superlubricity of RTILs under high normal loads must be investigated.

Recently, as depicted in **Figure 9**, researchers explored the robust superlubricity of a 1-ethyl-3-methylimidazolium trifluoromethanesulfonate ([EMIM]TFS) aqueous solution between a Si_3N_4/SiO_2 tribopair (Ge et al., 2018b). A COF as low as 0.002 was achieved under neutral conditions (pH $\approx$ 6.9 $\pm$ 0.1). Surface analysis shows that a tribochemical layer is deposited on the contact surfaces and provides low friction. This tribochemical layer is formed by tribochemical reactions and

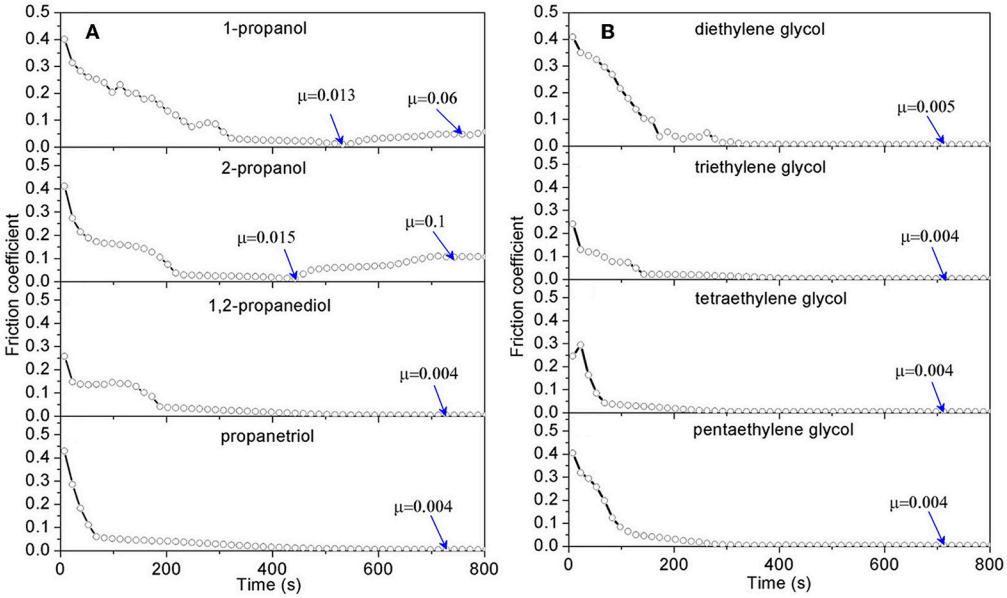

FIGURE 7 | COF under lubrication with mixtures of H_2SO_4 solution and polyhydroxy alcohols **(A)** with 3 carbon atoms in its carbon chain; **(B)** with various carbon chain length. The volume ratio of the polyhydroxy alcohols to the H_2SO_4 solution (pH 1) is 10:1. Li et al. (2013c) Copyright 2013, American Chemical Society.

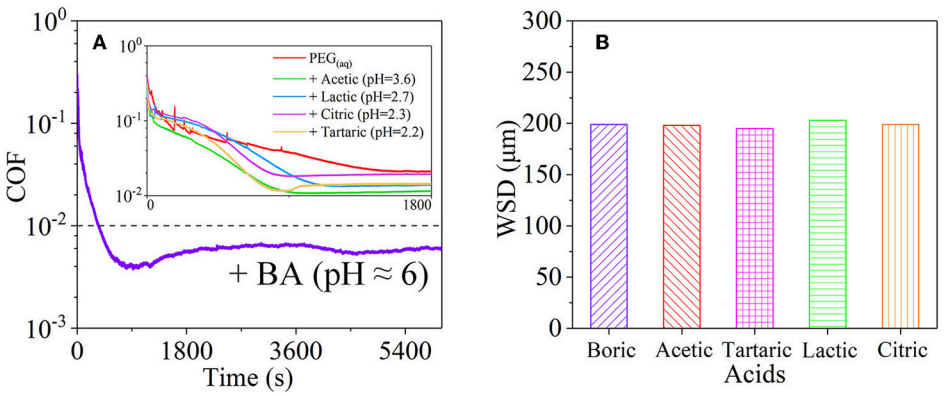

FIGURE 8 | (A) COFs and **(B)** wear scar diameter (WSD) of the mixtures of PEG and several acids: BA, acetic acid, tartaric acid, lactic acid, and citric acid. Ge et al. (2018a) Copyright 2018, American Chemical Society.

comprises [EMIM]TFS, colloidal silica, ammonia-containing compounds, and sulfides. Moreover, a fluid layer between the contact surfaces provides a low shear resistance. Because it has the superlubricity property under neutral conditions, [EMIM]TFS has great potential in engineering applications. Notably, RTILs can be designed by combining various cations and anions, giving rise to numerous potential RTILs with the superlubricity property. Nevertheless, the search for RTILs with the superlubricity property is in an initial stage, and additional research on the physicochemical and superlubricity properties is required.

OIL-BASED LUBRICANTS

In general, friction for liquid lubrication depends on the lubrication regime, which transitions from BL to ML and then to EHL. Moreover, the liquid friction is generally the lowest during the transition to EHL, where the thickness of the fluid film is perfect for separating the surfaces completely and providing extremely low viscous friction (Baykara et al., 2018). However, for viscous lubricants, such as oils and polyhydroxy alcohols, the COFs during EHL are ~0.05, which is higher than the maximum value for superlubricity (0.01). Therefore, surface modification of the tribopair is performed to make the surface interact with the viscous lubricants. One of the effective methods for modifying the contact surfaces is surface coating. Superlubricity has been observed for the tetrahedral amorphous carbon (ta-C) coating [a type of hydrogen-free diamond-like carbon (DLC)] under lubrication with poly-alpha-olefin (PAO), glycerol mono-oleate (GMO), and glycerol under BL (Kano, 2006a,b). The ta-C/steel tribopair shows an extremely low COF of 0.006 under lubrication with PAO + GMO at a sliding velocity of 100 mm/s, while

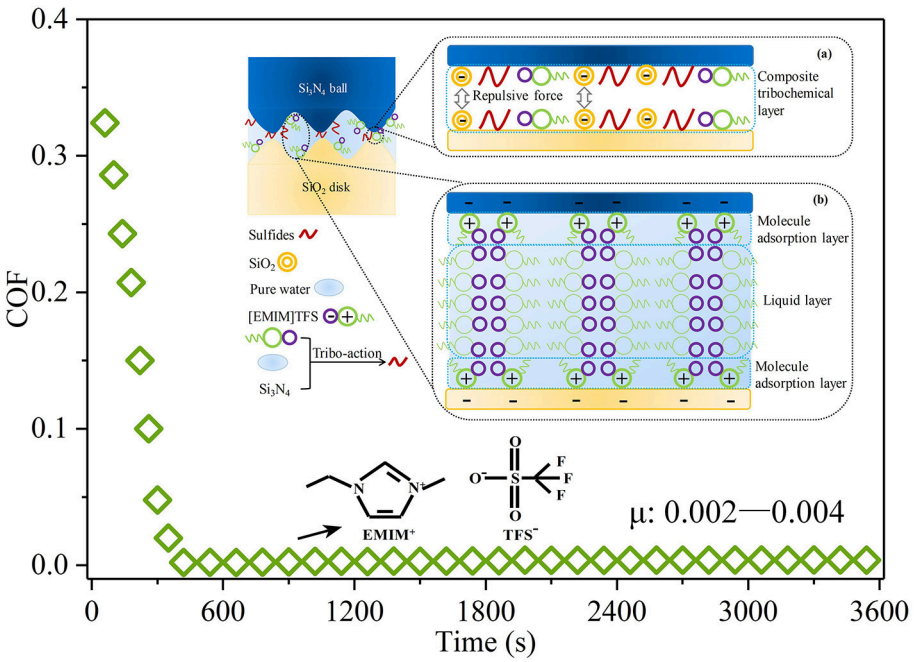

FIGURE 9 | COF of the [EMIM]TFS aqueous solution. The inset shows the proposed superlubricity model. Ge et al. (2018b) Copyright 2018, American Chemical Society.

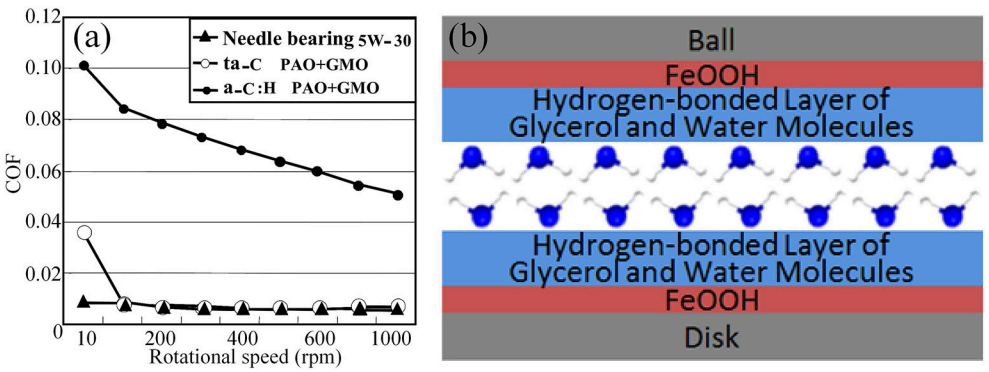

FIGURE 10 | (a) Relationship between the COF and the rotational speed. Bouchet et al. (2007) Copyright 2007, IOP Publishing Ltd. **(b)** Schematic of the lubrication model and molecular schematic presentation of the hydrogen-bond layer of glycerol and water. Chen et al. (2013) Copyright 2013, American Chemical Society.

the COF of a hydrogen-containing DLC/steel tribopair is >0.05, as depicted in **Figure 10a**. The superlubricity of the ta-C/ta-C tribopair is also achieved under lubrication with glycerol at 80°C (Bouchet et al., 2007; Matta et al., 2008). The computer simulation results show that OH atoms are nearly all bound to surface sp^1 atoms, resulting in the easy sliding property of this triboformed OH-terminated surfaces (Bouchet et al., 2007). At a low temperature, the superlubricity is also associated with the decomposition of glycerol, which generates a thin layer of organic acids and water, and the formation of a hydrogen-bond network (Matta et al., 2008). A similar mechanism applies for the superlubricity of the steel/steel tribopair under lubrication with a mixture of glycerol and *myo*-inositol (Matta et al., 2008), as well as aqueous glycerol (Chen et al., 2013), as depicted in **Figure 10b**. Notably, the lubrication with glycerol + *myo*-inositol yielded the first achievement of superlubricity in the absence of long-chain polar molecules under BL.

In addition to surface coating, alloys are typically used in mechanical engineering applications for different conditions. Some alloy tribopairs, such as Nitinol 60 alloy/steel tribopairs, are also used to study superlubricity. Superlubricity can be achieved under lubrication with castor oil in the boundary regime. Researchers examined the influence of the sliding speeds and normal loads on the friction in detail (Zeng and Dong, 2013). The results showed that the influence of the sliding speed on the lubricity is greater than that of the load owing to the

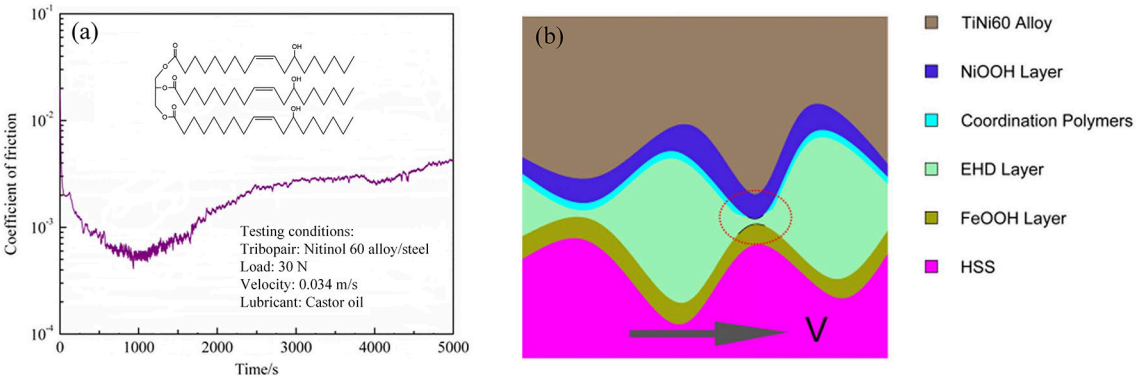

FIGURE 11 | (a) Evolution of the COF with time. The inset shows the main chemical structure of castor oil. **(b)** Lubrication diagrammatic sketch of the tribopair under castor-oil lubrication. Zeng et al. (2016) Copyright 2016, Nature.

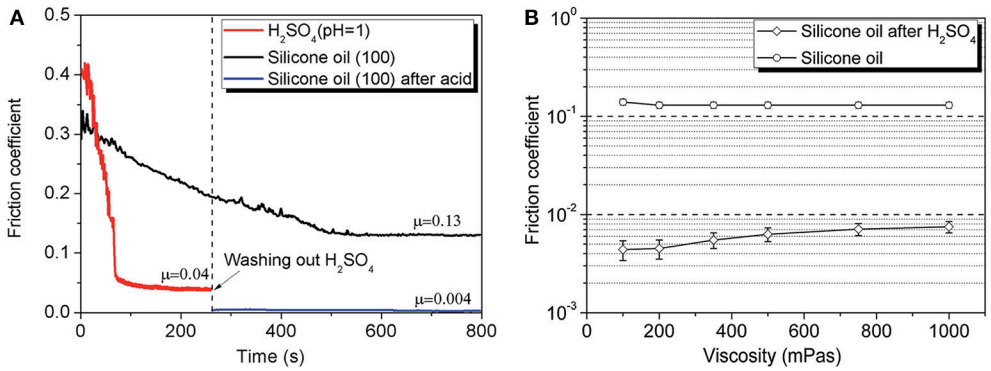

FIGURE 12 | (A) COF under lubrication with 100 mPa·s silicone oil, H_2SO_4 (pH = 1), and 100 mPa·s silicone oil after wearing-in with H_2SO_4 (pH = 1). **(B)** Final COF of silicone oils between the original surfaces (Si_3N_4/glass) and the surfaces after wearing-in with H_2SO_4 (pH = 1). The error bars represent the standard deviations of five measured values. Li et al. (2015a) Copyright 2015, the Royal Society of Chemistry.

chemical structure of castor oil, which is not suitable at high sliding speeds, because of its poor oxidation stability. Therefore, maintaining the sliding speed in an appropriate range is very important for achieving the superlubricity of the Nitinol 60 alloy. The same researchers compared castor oil, turbine oil, seed oil, and paraffin oil, and the results showed that only castor oil can achieve superlubricity for a Nitinol 60 alloy/steel tribopair (Zeng and Dong, 2014). Therefore, the hydroxyl groups branched on the acid chain may be necessary for superlubricity. The main chemical structure of castor oil has three long-chain fatty acids with an alkyl ester group, as depicted in the inset of **Figure 11a**. Thus, castor oil has the ability to form a thin film as an intermolecular layer and reduces the friction between the interfaces (Zeng and Dong, 2013). Analysis shows that tribochemical reactions occur during rubbing motion, including the decomposition of castor oil, the formation of iron oxy-hydroxide, and the triboformed OH-terminated surface with iron oxy-hydroxide. The authors propose a new superlubricity model, as depicted in **Figure 11b**. Here, a lamellar structure is formed by the intercalation of hexanoic acid molecules between Ni and iron oxy-hydroxide, which can provide strong repulsive electrostatic forces, contributing to the achievement of the superlubricity state (Zeng et al., 2016). As a good vegetable oil, castor oil is an eco-friendly lubricant owing to its excellent properties, such as its high biodegradability, renewability, and superlubricity performance. Therefore, the superlubricity achieved with castor oil makes it suitable for practical engineering applications in many fields, including biotechnology.

Researchers also achieved superlubricity with silicone oil between a Si_3N_4/glass tribopair by pre-treating the interface with H_2SO_4 (Li et al., 2015a). The COF of silicone oils can decrease to as low as 0.004, which is only 1/30 of its original value (0.13), as depicted in **Figure 12**. The acid helps to form a plane on the ball and a micro-slope on the disc, leading to the reduction of the contact pressure during the wearing-in period. The silicone oil helps to form a hydrodynamic layer between the contact surfaces. The tribochemical reaction between Si_3N_4 and water provides a low friction in ML but hardly affects the friction in EHL. The liquid superlubricity achieved with silicone oil accounts for the formation of ML and EHL between the plane on the ball and the micro-slope on the disc, which are formed

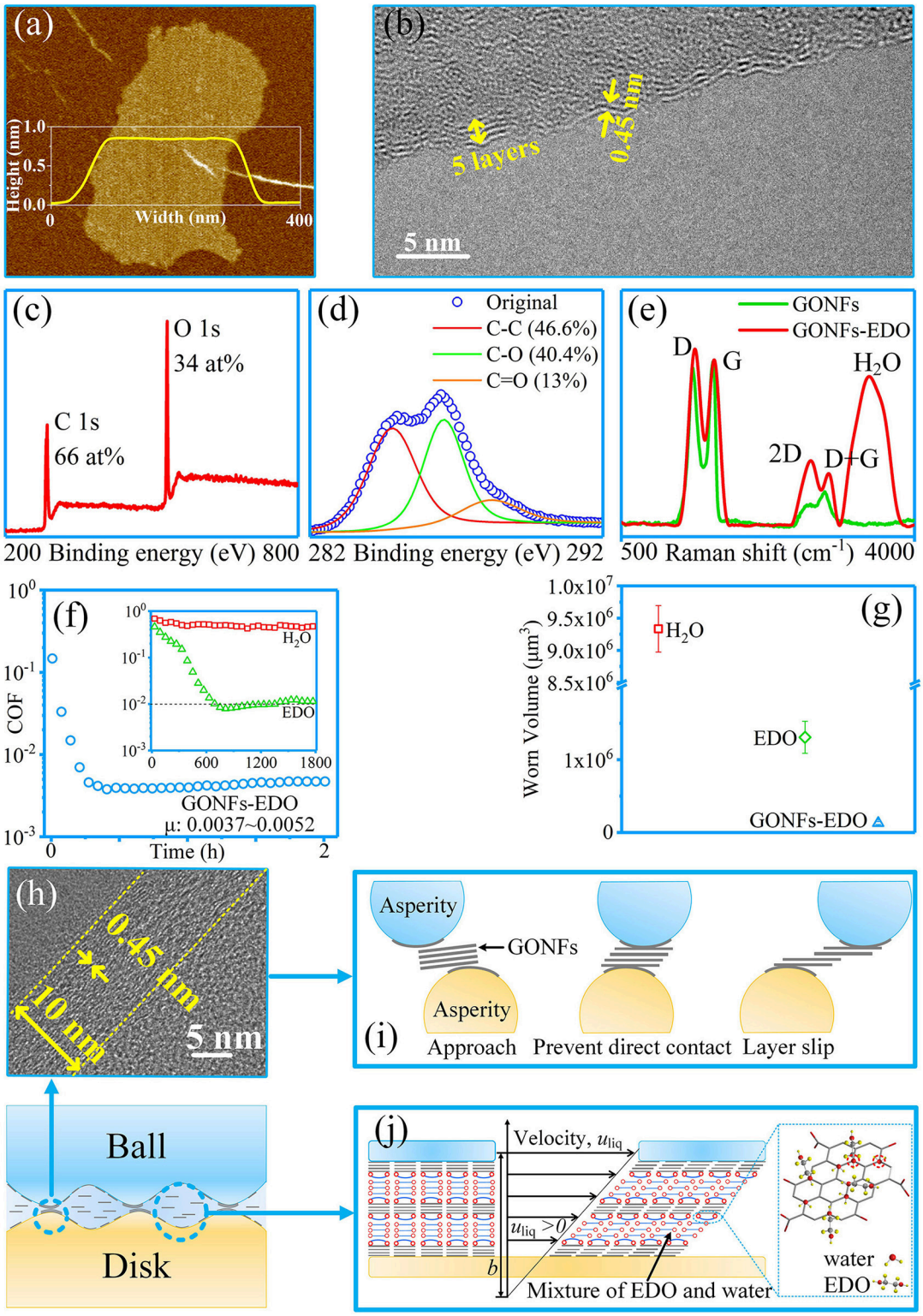

FIGURE 13 | Characterization of GONFs: **(a)** atomic force microscopy image; **(b)** high-resolution transmission electron microscopy (HRTEM) image; **(c,d)** XPS spectra; **(e)** Raman spectra. **(f,g)** Friction and wear testing results for GONFs-EDO. **(h)** HRTEM image of the cross-sectional area of the worn surface. **(i,j)** Proposed superlubricity and anti-wear mechanism of GONFs-EDO. Ge et al. (2018d) Copyright 2018, American Chemical Society.

during the wearing-in period with acid. Later, the same authors found that this kind of superlubricity cannot be achieved at a sapphire/sapphire tribopair when the average contact pressure is >50 MPa (Li et al., 2015b). The authors demonstrated via calculation that this kind of liquid superlubricity is related to both the contact pressure between the contact surfaces and the pressure–viscosity coefficient (PVC) of the lubricant. Their calculation results show that under a high contact pressure, the PVC must be as small as possible to achieve superlubricity, whereas under a low contact pressure, superlubricity can be achieved in a wide range of PVCs. Most recently, our group achieved superlubricity with both polar (polyalkylene glycols (PAG) and non-polar (PAO) oils between a steel/steel tribopair by pre-treating the interface with $PEG_{(aq)}$ (Ge et al., 2018c). The superlubricity was found to achieve at thin film lubrication regime (Gao et al., 2018; Qiao et al., 2018), which is composed of a tribochemical layer (formed by the tribochemical reaction between PEG and steel surfaces), an ordered layer (formed by the PAG or PAO molecules), and a liquid film of the lubricants.

NANOMATERIAL-BASED LUBRICANTS

One common feature of liquid superlubricity is that a wearing-in process is required before the achievement of superlubricity, which usually leads to severe wear. It has been proven that graphene-oxide (GO) materials can provide wear protection. Through the generation of a GO-adsorption film on the contact surfaces, GO can separate the contact surfaces and reduce the wear (Wu et al., 2018; Zhao et al., 2018). However, the macroscale COFs of GO are generally in the range of 0.02–0.1 (Meng et al., 2015; Jaiswal et al., 2016; Fan et al., 2018; Wu et al., 2018; Zhang et al., 2018; Zhao et al., 2018), indicating a near-superlubricity state or traditional lubrication state.

Our group achieved a macroscale superlubricity state through the synergy effect of GONFs and ethanediol (EDO) at ceramic tribopairs including Si_3N_4/SiO_2, Si_3N_4/Si_3N_4, and Si_3N_4/Sapphire (Ge et al., 2018d). The used GONFs were prepared via a modified Hummers method. They were 0.8 nm thick, had an interlayer spacing of 0.45 nm, and had an oxygen content of 30–40%, as depicted in **Figures 13a–e**. The results for the friction and wear of GONFs-EDO are depicted in **Figures 13f,g**. The COF of GONFs-EDO decreased to <0.01 after the wearing-in period of 600 s; thereafter, the COF further decreased to 0.0037 and remained stable for 2 h. Furthermore, the wear results show that the wear volume of the ball under lubrication with GONFs-EDO (5.1×10^4 μm^3) was only 5% of that of the ball under lubrication with EDO (1.3×10^6 μm^3). These results indicate the excellent superlubricity and anti-wear performances of GONFs-EDO. GONFs were adsorbed on the surfaces of the tribopair (**Figure 13h**), preventing direct contact between asperities. The super-low shear stresses between the GONFs interfaces contributed to the superlubricity and super-low wear, as depicted in **Figure 13i**. Moreover, the formation of the GONFs-EDO hydrated network and the partial-slip boundary condition at the GONFs-EDO interface contributed to the super-low shear stresses of the liquid layer, leading to superlubricity, as depicted in **Figure 13j**.

Other nanomaterials like BP-OH, BN, LDH, and nanodiamonds were also found to help the base lubricants achieve superlubricity. The superlubricity mechanism for BP-OH aqueous solution is attributed to the effective lubricating layer formed by the attachment of water molecules on BP-OH nanosheets in the silica-gel (Wang et al., 2018). The superlubricity mechanism for BN-containing PAO at Si_3N_4/DLC interface is the contact area reduction because of BN as nanoscale ball bearings lead to the point-like contact, and the weak van der Waals interaction force between BN molecules (Zeng et al., 2013). The superlubricity mechanism for LDH is regarded as its small size and good dispersion in water make LDH enter the contact area and form an effective lubricating layer, and therefore protect the asperity peaks from direct collision (Wang et al., 2016). Additionally, nanodiamonds glycerol colloidal solution was found to achieve superlubricity and low wear, which are due to the hydrodynamic effect, hydrogen bond layer, and rolling effect of nanodiamonds (Chen et al., 2016).

CONCLUSIONS AND OUTLOOKS

Studies on liquid superlubricity at the macroscale are focused on the mechanism, which differs for different lubricants and is usually attributed to multiple factors, such as the silica layers and hydrodynamic lubrication for water, the tribochemical layer, and hydrogen-bond network for viscous lubricants, and the stern layer and hydrogen-bond network for acid-based lubricants. The mechanism of liquid superlubricity is very complicated and should be further investigated. Because of the limitation of the present technology, the structure, and arrangement of liquid molecules in the contact region, which play the dominate role on the superlubricity, are still not clear. In addition, the kinds of materials for liquid superlubricity are limited; only a few materials exhibit superlubricity behavior. The possibility of other liquid materials with superlubricity properties remains to be investigated. Furthermore, there are many factors that limit the application of liquid superlubricity, such as the severe wear, acidic conditions, and complexity of manufacturing ideal surfaces. However, the prospects for liquid superlubricity in industrial applications are excellent. For instance, hydrophilic polymer brushes may be suitable for silicone rubbers in microfluidics, marine paints (antifouling), biomedical devices, etc. Acid-based lubricants and ionic liquids may be suitable for Si_3N_4 bearings, who have strong resistance to acidic corrosion. Oil-based lubricants may be suitable for the mechanical parts like gears and bearings, who are made of steels and alloys. PVPA-modified Ti_6Al_4V is a potential material for artificial implants. Therefore, research in the near future should focus on the development of new liquid lubricants to offer lubricating performance with extremely low friction and wear, as well as be associated with practical operating conditions in mechanical systems.

AUTHOR CONTRIBUTIONS

JLu and JLi gave the guidance on the structure and content of this review. XGe completed this review.

ACKNOWLEDGMENTS

The work is financially supported by the National Natural Science Foundation of China (51775295, 51527901, and 51335005).

REFERENCES

Baykara, M., Vazirisereshk, M., and Martini, A. (2018). Emerging superlubricity: a review of the state of the art and perspectives on future research. *Appl. Phys. Rev*. 5:041102. doi: 10.1063/1.5051445

Berman, D., Erdemir, A., and Sumant, A. (2018). Approaches for achieving superlubricity in two-dimensional materials. *ACS Nano* 12, 2122–2137. doi: 10.1021/Acsnano.7b09046

Bouchet, M., Matta, C., Le-Mogne, T., Martin, J., Zhang, Q., Goddard, W., et al. (2007). Superlubricity mechanism of diamond-like carbon with glycerol. Coupling of experimental and simulation studies. *J. Phys. Confer. Ser.* 89:012003. doi: 10.1088/1742-6596/89/1/012003

Chen, M., Kato, K., and Adachi, K. (2001). The difference in running-in period and friction coefficient between self-mated Si3N4 and SiC under water lubrication. *Tribol. Lett*. 11, 23–28. doi: 10.1023/A:1016621929078

Chen, M., Kato, K., and Adachi, K. (2002). The comparisons of sliding speed and normal load effect on friction coefficients of self-mated Si3N4 and SiC under water lubrication. *Tribol. Int*. 35, 129–135. doi: 10.1016/S0301-679X(01)00105-0

Chen, Z., Liu, Y., and Luo, J. (2016). Superlubricity of nanodiamonds glycerol colloidal solution between steel surfaces. *Colloids Surf. A* 489, 400–406. doi: 10.1016/j.Colsurfa.2015.10.062

Chen, Z., Liu, Y., Zhang, S., and Luo, J. (2013). Controllable super lubricity of glycerol solution via environment humidity. *Langmuir* 29, 11924–11930. doi: 10.1021/La402422h

Cihan, E., Ipek, S., Durgun, E., and Baykara, M. (2016). Structural lubricity under ambient conditions. *Nat. Commun*. 7:12055. doi: 10.1038/Ncomms12055

Dash, J., Fu, H., and Wettlaufer, J. (1995). The premelting of ice and its environmental consequences. *Rep. Prog. Phys*. 58, 115–167. doi: 10.1088/0034-4885/58/1/003

Deng, M., Zhang, C., Li, J., Ma, L., and Luo, J. (2014). Hydrodynamic effect on the superlubricity of phosphoric acid between ceramic and sapphire. *Friction* 2, 173–181. doi: 10.1007/S40544-014-0053-3

Erdemir, A., and Eryilmaz, O. (2014). Achieving superlubricity in DLC films by controlling bulk, surf ace, and tribochemistry. *Friction* 2, 140–155. doi: 10.1007/S40544-014-0055-1

Erdemir, A., and Martin, J., (eds.). (2007). *Superlubricity*. New York, NY: Elsvier. doi: 10.1016/B978-0-444-52772-1.X5029-X

Espinosa, T., Jimenez, M., Sanes, J., Jimenez, A., Iglesias, M., and Bermudez, M. (2014). Ultra-low friction with a protic ionic liquid boundary film at the water-lubricated sapphire-stainless steel interface. *Tribol. Lett*. 53, 1–9. doi: 10.1007/S11249-013-0238-3

Fan, K., Liu, J., Wang, X., Liu, Y., Lai, W., Gao, S., et al. (2018). Towards enhanced tribological performance as water-based lubricant additive: selective fluorination of graphene oxide at mild temperature. *J. Colloid Interf. Sci*. 531, 138–147. doi: 10.1016/j.Jcis.2018.07.059

Fan, M., Song, Z., Liang, Y., Zhou, F., and Liu, W. (2014). Laxative inspired ionic liquid lubricants with good detergency and no corrosion. *ACS Appl. Mater. Interfaces* 6, 3233–3241. doi: 10.1021/Am4049332

Feng, X., Kwon, S., Park, J., and Salmeron, M. (2013). Superlubric sliding of graphene nanoflakes on graphene. *ACS Nano* 7, 1718–1724. doi: 10.1021/Nn305722d

Gao, M., Li, H., Ma, L., Gao, Y., Ma, L., and Luo, J. (2018). "Molecular behaviors in thin film lubrication, part two: direct observation of the molecular orientation near the solid surface,"in *Friction Accepted*, ed J. Luo (Beijing: Tsinghua University Press).

Ge, X., Halmans, T., Li, J., and Luo, J. (2018c). "Molecular behaviors in thin film lubrication, part three: superlubricity attained by polar and nonpolar molecules," *Friction Online*, ed J. Luo (Beijing: Tsinghua University Press). doi: 10.1007/S40544-018-0254-2

Ge, X., Li, J., Luo, R., Zhang, C., and Luo, J. (2018d). Macroscale superlubricity enabled by synergy effect of graphene-oxide nanoflakes and ethanediol. *ACS Appl. Mater. Interfaces* 10, 40863–40870. doi: 10.1021/Acsami.8b14791

Ge, X., Li, J., Zhang, C., and Luo, J. (2018a). Liquid superlubricity of polyethylene glycol aqueous solution achieved with boric acid additive. *Langmuir* 34, 3578–3587. doi: 10.1021/acs.Langmuir.7b04113

Ge, X., Li, J., Zhang, C., Wang, Z., and Luo, J. (2018b). Superlubricity of 1-ethyl-3-methylimidazolium trifluoromethanesulfonate ionic liquid induced by tribochemical reactions. *Langmuir* 34, 5245–5252. doi: 10.1021/acs.Langmuir.8b00867

Ge, X., Xia, Y., and Shu, Z. (2015). Conductive and tribological properties of lithium-based ionic liquids as grease base oil. *J. Tribol. Trans. ASME* 58, 686–690. doi: 10.1080/10402004.2015.1012772

Han, T., Zhang, C., and Luo, J. (2018). Macroscale superlubricity enabled by hydrated alkali metal ions. *Langmuir* 34, 11281–11291. doi: 10.1021/acs.Langmuir.8b01722

Hirano, M. (2014). Atomistics of superlubricity. *Friction* 2, 95–105. doi: 10.1007/S40544-014-0049-Z

Holmberg, K., Andersson, P., and Erdemir, A. (2012). Global energy consumption due to friction in passenger cars. *Tribol. Int*. 47, 221–234. doi: 10.1016/j.Triboint.2011.11.022

Inutsuka, M., Yamada, N., Ito, K., and Yokoyama, H. (2013). High density polymer brush spontaneously formed by the segregation of amphiphilic diblock copolymers to the polymer/water interface. *ACS Macro Lett*. 2, 265–268. doi: 10.1021/Mz300669q

Jaiswal, V., Kalyani., Umrao, S., Rastogi, R., Kumar, R., and Srivastava, A. (2016). Synthesis, characterization, and tribological evaluation of TiO2-reinforced boron and nitrogen co-doped reduced graphene oxide based hybrid nanomaterials as efficient antiwear lubricant additives. *ACS Appl. Mater. Interfaces* 8, 11698–11710. doi: 10.1021/Acsami.6b01876

Jiang, C., Li, W., Nian, J., Lou, W., and Wang, X. (2018). Tribological evaluation of environmentally friendly ionic liquids derived from renewable biomaterials. *Friction* 6, 208–218. doi: 10.1007/S40544-017-0170-X

Kano, M. (2006a). DLC coating technology applied to sliding parts of automotive engine. *New Diamond Front. Carbon Technol*. 16, 201–210.

Kano, M. (2006b). Super low friction of DLC applied to engine cam follower lubricated with ester-containing oil. *Tribol. Int*. 39, 1682–1685. doi: 10.1016/j.Triboint.2006.02.068

Kawai, S., Benassi, A., Gnecco, E., Söde, H., Pawlak, R., Feng, X., et al. (2016). Superlubricity of graphene nanoribbons on gold surfaces. *Science* 351, 957–961. doi: 10.1126/Science.Aad3569

Khajeh, A., He, X., Yeon, J., Kim, S., and Martini, S. (2018). Mechanochemical association reaction of interfacial molecules driven by shear. *Langmuir* 34, 5971–5977. doi: 10.1021/acs.Langmuir.8b00315

Klein, J. (2013). Hydration lubrication. *Friction* 1, 1–23. doi: 10.1007/S40544-013-0001-7

Lee, S., Muller, M., Ratoi-Salagean, M., Voros, J., Pasche, S., De Paul, S., et al. (2003). Boundary lubrication of oxide surfaces by Poly(L-Lysine)-G-Poly(Ethylene Glycol) (PLL-G-PEG) in aqueous media. *Tribol. Lett*. 15, 231–239. doi: 10.1023/A:1024861119372

Li, H., Wood, R., Rutland, M., and Atkin, R. (2014). An ionic liquid lubricant enables superlubricity to be "Switched on" *in situ* using an electrical potential. *Chem. Commun*. 50, 4368–4370. doi: 10.1039/C4cc00979g

Li, J., Gao, T., and Luo, J. (2018a). Superlubricity of graphite induced by multiple transferred graphene nanoflakes. *Adv. Sci*. 5:1700616. doi: 10.1002/Advs.201700616

Li, J., Ge, X., and Luo, J. (2018b). Random occurrence of macroscale superlubricity of graphite enabled by tribo-transfer of multilayer graphene nanoflakes. *Carbon* 138, 154–160. doi: 10.1016/j.Carbon.2018.06.001

Li, J., Ma, L., Zhang, S., Zhang, C., Liu, Y., and Luo, J. (2013a). Investigations on the mechanism of superlubricity achieved with phosphoric acid solution by direct observation. *J. Appl. Phys*. 114:114901. doi: 10.1063/1.4821063

Li, J., Zhang, C., Deng, M., and Luo, J. (2014). Investigations of the superlubricity of sapphire against ruby under phosphoric acid lubrication. *Friction* 2, 164–172. doi: 10.1007/S40544-014-0050-6

Li, J., Zhang, C., Deng, M., and Luo, J. (2015a). Superlubricity of silicone oil achieved between two surfaces by running-in with acid solution. *RSC Adv*. 5, 30861–30868. doi: 10.1039/C5ra00323g

Li, J., Zhang, C., Deng, M., and Luo, J. (2015b). Investigation of the difference in liquid superlubricity between water- and oil-based lubricants. *RSC Adv*. 5, 63827–63833. doi: 10.1039/C5ra10834a

Li, J., Zhang, C., and Luo, J. (2011). Superlubricity behavior with phosphoric acid-water network induced by rubbing. *Langmuir* 27, 9413–9417. doi: 10.1021/La201535x

Li, J., Zhang, C., and Luo, J. (2013c). Superlubricity achieved with mixtures of polyhydroxy alcohols and acids. *Langmuir* 29, 5239–5245. doi: 10.1021/La400810c

Li, J., Zhang, C., Ma, L., Liu, Y., and Luo, J. (2013b). Superlubricity achieved with mixtures of acids and glycerol. *Langmuir* 29, 271–275. doi: 10.1021/La3046115

Li, J., Zhang, C., Sun, L., Lu, X., and Luo, J. (2012). Tribochemistry and superlubricity induced by hydrogen ions. *Langmuir* 28, 15816–15823. doi: 10.1021/La303897x

Li, Y., Zhang, S., Ding, Q., Feng, D., Qin, B., and Hu, L. (2017). The corrosion and lubrication properties of 2-mercaptobenzothiazole functionalized ionic liquids for bronze. *Tribol. Int*. 114, 121–131. doi: 10.1016/j.Triboint.2017.04.022

Liu, Z., Yang, J., Grey, F., Liu, J., Liu, Y., Wang, Y., et al. (2012). Observation of microscale superlubricity in graphite. *Phys. Rev. Lett*. 108:205503. doi: 10.1103/PhysRevLett.108.205503

Ma, W., Gong, Z., Gao, K., Qiang, L., Zhang, J., and Yu, S. (2017). Superlubricity achieved by carbon quantum dots in ionic liquid. *Mater. Lett*. 195, 220–223. doi: 10.1016/j.Matlet.2017.02.135

Martin, J., Pascal, H., Donnet, C., Le Mogne, T., Loubet, J., and Epicier, T. (1994). Superlubricity of MoS2: crystal orientation mechanisms. *Surf. Coat. Technol*. 68–69, 427–432. doi: 10.1016/0257-8972(94)90197-X

Matta, C., Joly-Pottuz, L., Bouchet, M., and Martin, J. (2008). Superlubricity and tribochemistry of polyhydric alcohols. *Phys. Rev. B* 78:085436. doi: 10.1103/PhysRevB.78.085436

Meng, Y., Su, F., and Chen, Y. (2015). A novel nanomaterial of graphene oxide dotted with Ni nanoparticles produced by supercritical CO2-assisted deposition for reducing friction and wear. *ACS Appl. Mater. Interfaces* 7, 11604–11612. doi: 10.1021/Acsami.5b02650

Meyer, E., and Gnecco, E. (2014). Superlubricity on the nanometer scale. *Friction* 2, 106–113. doi: 10.1007/S40544-014-0052-4

Muller, M., Lee, S., Spikes, H., and Spencer, N. (2003). The influence of molecular architecture on the macroscopic lubrication properties of the brush-like co-polyelectrolyte poly(L-Lysine)-G-poly(Ethylene Glycol) (PLL-G-PEG) adsorbed on oxide surfaces. *Tribol. Lett*. 15, 395–405. doi: 10.1023/B:TRIL.0000003063.98583.bb

Qiao, Y., Zhang, S., Liu, Y., Ma, L., and Luo, J. (2018). "Molecular behaviors in thin film lubrication, part one: film formation for different polarities of molecules,"in *Friction Submitted*, ed J. Luo (Beijing: Tsinghua University Press).

Qu, J., Bansal, D., Yu, B., Howe, J. Y., Luo, H., Dai, S., et al. (2012). Antiwear performance and mechanism of an oil-miscible ionic liquid as a lubricant additive. *ACS Appl. Mater. Interfaces* 4, 997–1002. doi: 10.1021/Am201646k

Qu, J., Barnhill, W., Luo, H., Meyer, H., Leonard, D., Landauer, A., et al. (2015). Synergistic effects between phosphonium-alkylphosphate ionic liquids and zinc dialkyldithiophosphate (ZDDP) as lubricant additives. *Adv. Mater*. 27, 4767–4774. doi: 10.1002/Adma.201502037

Raviv, U., Giasson, S., Kampf, N., Gohy, J., Jerome, R., and Klein, J. (2003). Lubrication by charged polymers. *Nature* 425, 163–165. doi: 10.1038/Nature01970

Ron, T., Javakhishvili, I., Hvilsted, S., Jankova, K., and Lee, S. (2016). Ultralow friction with hydrophilic polymer brushes in water as segregated from silicone matrix. *Adv. Mater. Interfaces* 3:1500472. doi: 10.1002/Admi.201500472

Sahai, N. (2002). Is silica really an anomalous oxide? Surface acidity and aqueous hydrolysis revisited. *Environ. Sci. Technol*. 36, 445–452. doi: 10.1021/Es010850u

Saurin, N., Sanes, J., Carrion, F., and Bermudez, M. (2016). Self-healing of abrasion damage on epoxy resin controlled by ionic liquid. *RSC Adv*. 6, 37258–37264. doi: 10.1039/C6ra05503f

Shinjo, K., and Hirano, M. (1993). Dynamics of friction-superlubric state. *Surf. Sci*. 283, 473–478. doi: 10.1016/0039-6028(93)91022-H

Shteinberg, L. (2009). Effect of boric acid concentration on the catalysis of the reaction of 4-nitrobenzoic acid with ammonia. *Russ. J. Appl. Chem*. 82, 613–617. doi: 10.1134/S1070427209040156

Shteinberg, L. (2011). A study of the kinetics and mechanism of amidation of 4-nitrobenzoic acid with ammonia, catalyzed by boric acid in the presence of polyethylene glycol PEG-400. *Russ. J. Appl. Chem*. 84, 815–819. doi: 10.1134/S1070427211050132

Sinclair, R. C., Suter, J. L., and Coveney, P. V. (2018). Graphene–graphene interactions: friction, superlubricity, and exfoliation. *Adv. Mater*. 30:1705791. doi: 10.1002/Adma.201705791

Sjoberg, S. (1996). Silica in aqueous environments. *J. Non-Cryst. Solids* 196, 51–57. doi: 10.1016/0022-3093(95)00562-5

Somers, A., Khemchandani, B., Howlett, P., Sun, J., MacFarlane, D., and Forsyth, M. (2013). Ionic liquids as antiwear additives in base oils: influence of structure on miscibility and antiwear performance for steel on aluminum. *ACS Appl. Mater. Interfaces* 5, 11544–11553. doi: 10.1021/Am4037614

Song, Y., Mandelli, D., Hod, O., Urbakh, M., Ma, M., and Zheng, Q. (2018). Robust microscale superlubricity in graphite/hexagonal boron nitride layered heterojunctions. *Nat Mater*. 17, 894–899. doi: 10.1038/S41563-018-0144-Z

Spikes, H., and Tysoe, W. (2015). On the commonality between theoretical models for fluid and solid friction, wear and tribochemistry. *Tribol. Lett*. 59:21. doi: 10.1007/S11249-015-0544-Z

Tisza, L. (1938). On the thermal supraconductibility of liquid helium II and the bose-einstein statistics. *Comptes Rendus Hebdomadaires Des Seances De L'Academie Des Sci.* 207, 1035–1037.

Tomizawa, H., and Fischer, T. (1987). Friction and wear of silicon-nitride and silicon-carbide in water: hydrodynamic lubrication at low sliding speed obtained by tribochemical wear. *ASLE Trans*. 30, 41–46. doi: 10.1080/05698198708981728

Wang, H., Liu, Y., Chen, Z., Wu, B., Xu, S., and Luo, J. (2016). Layered double hydroxide nanoplatelets with excellent tribological properties under high contact pressure as water-based lubricant additives. *Sci. Rep*. 6:22748. doi: 10.1038/Srep22748

Wang, W., Xie, G., and Luo, J. (2018). Superlubricity of black phosphorus as lubricant additive. *ACS Appl. Mater. Interfaces* 10, 43203–43210. doi: 10.1021/Acsami.8b14730

Wang, X., Kato, K., Adachi, K., and Aizawa, K. (2001). The effect of laser texturing of SiC surface on the critical load for transition of water lubrication mode from hydrodynamic to mixed. *Tribol. Int*. 34, 703–711. doi: 10.1016/S0301-679X(01)00063-9

Wu, L., Xie, Z., Gu, L., Song, B., and Wang, L. (2018). Investigation of the tribological behavior of graphene oxide nanoplates as lubricant additives for ceramic/steel contact. *Tribol. Int*. 128, 113–120. doi: 10.1016/j.Triboint.2018.07.027

Xu, J., and Kato, K. (2000). Formation of tribochemical layer of ceramics sliding in water and its role for low friction. *Wear* 245, 61–75. doi: 10.1016/S0043-1648(00)00466-X

Ye, C., Liu, W., Chen, Y., and Yu, L. (2001). Room-temperature ionic liquids: a novel versatile lubricant. *Chem. Commun*. 2001, 2244–2245. doi: 10.1039/B106935g

Yue, D., Ma, T., Hu, Y., Yeon, J., van Duin, A., Wang, H., et al. (2013). Tribochemistry of phosphoric acid sheared between quartz surfaces: a reactive molecular dynamics study. *J. Phys. Chem. C* 117, 25604–25614. doi: 10.1021/Jp406360u

Zeng, Q., and Dong, G. (2013). Influence of load and sliding speed on super-low friction of nitinol 60 alloy under castor oil lubrication. *Tribol. Lett*. 52, 47–55. doi: 10.1007/S11249-013-0191-1

Zeng, Q., and Dong, G. (2014). Superlubricity behaviors of nitinol 60 alloy under oil lubrication. *Trans. Nonferrous Met. Soc. China* 24:354359. doi: 10.1016/S1003-6326(14)63068-5

Zeng, Q., Dong, G., and Martin, J. (2016). Green superlubricity of nitinol 60 alloy against steel in presence of castor oil. *Sci. Rep*. 6:29992. doi: 10.1038/Srep29992

Zeng, Q., Yu, F., and Dong, G. (2013). Superlubricity behaviors of Si3N4/DLC films under PAO oil with nano boron nitride additive lubrication. *Surf. Interface Anal.* 45, 1283–1290. doi: 10.1002/sia.5269

Zhang, C., Liu, Y., Liu, Z., Zhang, H., Cheng, Q., and Yang, C. (2017). Regulation mechanism of salt ions for superlubricity of hydrophilic polymer cross-linked networks on Ti6Al4V. *Langmuir* 33, 2133–2140. doi: 10.1021/acs.Langmuir.6b04429

Zhang, G., Xu, Y., Xiang, X., Zheng, G., Zeng, X., Li, Z., et al. (2018). Tribological performances of highly dispersed graphene oxide derivatives in vegetable oil. *Tribol. Int.* 126, 39–48. doi: 10.1016/j.Triboint.2018.05.004

Zhao, F., Zhang, L., Li, G., Guo, Y., Qi, M., and Zhang, G. (2018). Significantly enhancing tribological performance of epoxy by filling with ionic liquid functionalized graphene oxide. *Carbon* 136, 309–319. doi: 10.1016/j.Carbon.2018.05.002

Zhou, F., Adachi, K., and Kato, K. (2005). Friction and wear property of a-CNx coatings sliding against ceramic and steel balls in water. *Diam. Relat. Mater.* 14, 1711–1720. doi: 10.1016/j.Diamond.2005.06.025

Zhou, F., Wang, X., Kato, K., and Dai, Z. (2007). Friction and wear property of a-CNx coatings sliding against Si3N4 balls in water. *Wear* 263, 1253–1258. doi: 10.1016/j.Wear.2006.11.048

Conflict of Interest Statement: The authors declare that the research was conducted in the absence of any commercial or financial relationships that could be construed as a potential conflict of interest.